

On the process dependent nuclear k_{\perp} broadening effect

Andreas Schäfer and Jian Zhou

Institut für Theoretische Physik, Universität Regensburg, Regensburg, Germany

October 30, 2018

Abstract

We study the process dependent nuclear k_{\perp} broadening effect by employing the transverse momentum dependent (TMD) factorization approach in combination with the McLerran-Venugopalan (MV) model. More specifically, we investigate how the parton transverse momentum distributions are affected by the process dependent gauge links in cold nuclear matter. In particular, our analysis also applies to the polarized cases including the nuclear quark Boer-Mulders function and the linearly polarized gluon distribution. Our main focus is on the nuclear TMDs at intermediate or large x .

1 Introduction

The detailed understanding of the properties of hot and cold nuclear matter is one of the topical problems of QCD, in particular in connection with high energy heavy-ion experiments at RHIC, LHC and the future EIC. Initial/final state multiple parton re-scattering in a large nucleus plays an important role in revealing the properties of cold nuclear matter, as it leads to various physical effects, such as transverse momentum broadening of the propagating parton, parton energy loss due to induced gluon bremsstrahlung, and nuclear dependence of azimuthal asymmetries.

Much efforts have been devoted to the study of transverse momentum broadening in eA and pA collisions. A number of different approaches developed to describe this phenomenon were formulated within different theoretical frameworks, such as the eikonal approximation [1], twist-4 collinear factorization [2] and the resummation of higher twist contributions [3,4], dipole approach [5,6], the BDMPS formalism [7–9], diagrammatic Glauber multiple scattering [12], color glass condensate (CGC) effective theory [10,11], transverse momentum dependent factorization (TMD) [13], and soft collinear effective theory (SCET) [14–17]. The energy dependence of nuclear k_{\perp} broadening has also been investigated in Refs. [18,19].

Within the TMD factorization approach [20,21], we identified the gauge link appearing in the matrix element definition for nuclear TMDs as the main source of leading nuclear effects [13]. The formalism we developed in [13] was used to study k_{\perp} broadening as well as the nuclear dependence of azimuthal asymmetries [22–24] in semi-inclusive DIS (SIDIS) off a large nucleus. In SIDIS nuclear TMDs contain a future pointing gauge link describing the final state interactions, while a past pointing gauge link shows up in the nuclear TMDs associated with the Drell-Yan process in pA collisions due to initial state interactions. The contributions to k_{\perp} broadening from the future pointing and the past pointing gauge links are identical as this is a T-even observable. In the processes involving more complicated color flow, parton transverse momentum distributions can be affected by both initial and final state interactions, and thus could significantly differ from these in SIDIS and DY processes. The initial/final state interactions leading to k_{\perp} broadening in eA and pA collisions can be encoded in the various process dependent gauge links [25]. The purpose of this paper is to investigate the process

dependent nuclear TMDs at intermediate or large x following our general method described in [13]. As a byproduct, one can readily deduce k_{\perp} broadening simply by computing the k_{\perp}^2 moment of nuclear TMDs.

As a matter of fact, the process dependent nuclear TMDs at small x have been studied in both the unpolarized [26–28] and polarized cases [29, 30]. In general, small x nuclear TMDs associated with different hard scattering processes recover the same well known perturbative tail $1/k_{\perp}^2$ in the dilute medium limit, while they could differ significantly in the dense medium case where initial/final multiple re-scattering plays a more important role for parton transverse momentum spectra. One remarkable example is the difference between two widely used small x gluon TMDs in saturation physics: the Weizsäcker-Williams(WW) gluon distributions and the dipole gluon distribution. As pointed out in [27, 28], the WW gluon distribution contains a future pointing or past pointing gauge link in the adjoint representation while the dipole distribution contains a closed loop gauge link. Both gluon distributions can be probed in different hard scattering processes [27, 28].

In the present paper, we are aiming to extend the analyses [26–30] to the intermediate or large x region. At small x , TMDs are perturbatively calculable due to the presence of a semi-hard scale (the so called saturation scale), generated dynamically in high energy scattering. In contrast, nuclear TMDs at intermediate or large x can not be computed perturbatively. However, for the same reason, one can calculate contributions from initial/final state interactions encoded in process dependent gauge links in the MV model. By doing so, we are able to express nuclear TMDs as the convolution of the corresponding nucleon ones and process dependent small x gluon distributions. k_{\perp} broadening is obtained as byproduct from the relation between the nuclear TMD and the nucleon TMD in a specific hard scattering process.

At this point, we would like to briefly comment on the factorization properties of the relevant processes. Factorization in terms of TMDs containing process dependent gauge links is often referred to as generalized transverse momentum dependent(GTMD) factorization [25]. In the framework of GTMD factorization, the modified gauge links are obtained by resumming longitudinally polarized gluons into parton correlation functions on each nucleon side separately. However, recent work has shown that it is impossible to do so for di-jet production in pp collisions because the initial/final state interaction will not allow a separation of gauge links into the matrix elements of the various TMDs associated with each incoming proton. This has been explicitly illustrated by a concrete counter-example in Ref. [31]. In pA collisions, if one only takes into account the interaction between the active partons and the background gluon field inside a large nucleus while neglecting the longitudinal gluons attached to the proton side, the type of graph (for example Fig.11 in [31]) which can produce a violation of generalized TMD-factorization disappears. After neglecting the extra gluon attachment on the proton side, multiple gluon re-scattering between the hard part and the nucleus can be resummed to all orders in the form of a process dependent gauge link. As a result, the predictive power of the theory is partly restored in pA collisions.

We also noticed that the process dependent k_{\perp} broadening effect has been studied within the twist-4 collinear factorization approach [32–34]. The fact that the twist-4 collinear approach can be applied in the intermediate and large x region allows us to directly compare our formalism with the high-twist approach. It is shown that two approaches yield identical physical results for k_{\perp} broadening in different processes provided that the saturation scale and the twist-four quark gluon correlation functions are parameterized in a similar manner.

The paper is organized as follows: in Sec. 2, we review our general method developed in [13] and apply a modified version to compute the nuclear enhancement of the transverse momentum imbalance for quark pair production in eA collisions, and Drell-Yan di-lepton production in pA collisions. In addition, we establish relations between nuclear quark Boer-Mulders distributions and nucleon ones in SIDIS and Drell-Yan using the same approach. In Sec. 3, we study nuclear k_{\perp} broadening for

photon-jet production and quark pair production in pA collisions, respectively. In Sec. 4, we compare our results with those obtained in the collinear twist-4 approach and discuss the phenomenology implications. We conclude the paper and summarize our work in Sec. 5.

2 Nuclear TMDs in SIDIS and Drell-Yan

In our original work [13], multiple gluon correlations from the gauge link appearing in the definition of nuclear quark TMDs are reduced to products of nucleon small x gluon distribution in the so-called maximal two-gluon correlation approximation. From such expression, we obtained nuclear TMD as a convolution of a Gaussian distribution and a nucleon quark TMD. The width of the Gaussian is given by the gluon distribution density in the nuclear medium. However, the evaluation of Wilson lines in the MV model [35] has already reached a rather sophisticated level. In the present work, we will, therefore, compute the contribution from gauge links using the MV model instead of the maximal two-gluon correlation approximation. Both the unpolarized nuclear TMDs and the polarized TMDs (quark or gluon Boer-Mulders distributions) can be treated in the same framework. The resulting expression of the gauge link contribution in SIDIS computed in the MV model no longer has a Gaussian form once the finite nuclear matter size effect are taken into account. We start our derivation with the nuclear TMDs containing a simple future pointing or past pointing gauge link.

2.1 Semi-inclusive DIS scattering off a large nucleus

In this sub-section, we investigate how the out-going quark transverse momentum spectrum is affected by final state interactions encoded in the future pointing gauge link in the SIDIS process. The explicit relations between the nucleon quark TMDs and the corresponding nuclear ones are established.

Our starting point is the operator definition of quark TMDs in an unpolarized nucleon,

$$\begin{aligned} \mathcal{M}_N(x, \vec{k}_\perp) &= \int \frac{dr^- d^2 r_\perp}{(2\pi)^3} e^{ixP^+ r^- - i\vec{k}_\perp \cdot \vec{r}_\perp} \langle N | \bar{\psi}(y^-, y_\perp) U^{[+]} \psi(r^- + y^-, r_\perp + y_\perp) | N \rangle \\ &= \frac{1}{2} f_{1,DIS}(x, k_\perp) \not{p} + \frac{1}{2k_\perp} h_{1,DIS}^\perp(x, k_\perp) \sigma^{\mu\nu} k_\mu p_\nu, \end{aligned} \quad (1)$$

where k_\perp is defined as $k_\perp \equiv |\vec{k}_\perp|$, and p^μ is commonly defined light cone vector. The average over coordinate y is implied. $|N\rangle$ represents the nucleon state. $f_{1,DIS}(x, k_\perp)$ is the normal unpolarized quark distribution function containing a future pointing gauge link which arises from the final state interaction in the semi-inclusive DIS process. The second parton distribution $h_{1,DIS}^\perp(x, k_\perp)$ is commonly referred to as quark Boer-Mulders function [36]. Note that our convention for the quark Boer-Mulders function differs from the literatures [37–39] by a factor k_\perp/M_N , where M_N is target mass. Roughly speaking, the quark Boer-Mulders function describes the strength of the correlation between the quark transverse polarization and its transverse momentum. Color gauge invariance is ensured by two (future-pointing) gauge links in the fundamental representation,

$$U^{[+]} = \mathcal{P} e^{-ig \int_{y^-}^{\infty} d\zeta^- A^+(\zeta^-, y_\perp)} \mathcal{P} e^{-ig \int_{\infty}^{r^- + y^-} d\zeta^- A^+(\zeta^-, r_\perp + y_\perp)}. \quad (2)$$

We choose to work in the covariant gauge in which A^+ is the dominant component. The transverse pieces of the gauge link are suppressed and will be neglected in the derivation presented below [40].

Generally speaking, the longitudinal polarized gluons building up the gauge link may carry arbitrary collinear nucleon momentum fractions, since the gluon pole is not pinched. However, in this paper, we only focus on the contribution from small x gluons, which can be computed perturbatively

Figure 1: The ordinary future pointing gauge link is reduced to a short one by evaluating part of the gauge link stretching from R^- to ∞ in the MV model, where R^- is the radius of a nucleon.

due to the presence of a semi-hard scale Q_s . One might expect that the contribution to k_\perp broadening from gluons with large (or intermediate) longitudinal momentum fraction is suppressed as compared to that from small x gluons because of the high gluon number density at small x and the larger transverse momentum carried by these gluons.

Following a standard procedure (see, e.g., Ref. [41] for an overview), one first solves the classical Yang-Mills equation and obtains,

$$A_a^+(y^-, y_\perp) = -\frac{1}{\nabla_\perp^2} \rho_a(y^-, y_\perp), \quad (3)$$

where a is color index. We proceed by inserting this solution into the gauge link and averaging over the color sources $\rho(x^-, x_\perp)$ with the Gaussian distribution $W[\rho]$ [35].

$$W_A[\rho] = \exp \left\{ -\frac{1}{2} \int d^3 y \frac{\rho_a(y^-, y_\perp) \rho_a(y^-, y_\perp)}{\lambda_A(y^-)} \right\}, \quad (4)$$

where $\lambda_A(y^-)$ is the density of the color charges at a given y^- . With this ansatz for the distribution of color sources, the most elementary correlator is given by,

$$\begin{aligned} \langle A_a^+(y^-, y_\perp) A_b^+(r^-, r_\perp) \rangle &= \delta_{ab} \delta(y^- - r^-) \Gamma_A(y_\perp - r_\perp) \lambda_A(y^-) \\ \Gamma_A(k_\perp) &\equiv \frac{1}{k_\perp^4}. \end{aligned} \quad (5)$$

By repeatedly using this elementary correlator, one evaluates a pair of Wilson lines stretching from $y^- + R^-$ to infinity with R^- being the nucleon radius.

$$\begin{aligned} &\left\langle \left[\mathcal{P} e^{-ig \int_{y^-+R^-}^{\infty} d\zeta^- A^+(\zeta^-, y_\perp)} \mathcal{P} e^{-ig \int_{\infty}^{y^-+R^-} d\zeta^- A^+(r_\perp + y_\perp, \zeta^-)} \right]_{ab} \right\rangle \\ &= \exp \left\{ -C_F \Theta(r_\perp^2) \int_{R^-+y^-}^{\infty} d\zeta^- \lambda_A(\zeta^-) \right\} \delta_{ab}. \end{aligned} \quad (6)$$

where $\Theta(r_\perp^2) \equiv g^2 [\Gamma_A(0_\perp) - \Gamma_A(r_\perp)] \simeq g^2 \frac{r_\perp^2}{16\pi} \ln \frac{1}{r_\perp^2 \Lambda_{QCD}^2}$. Note that these two Wilson lines are connected in color space at infinity. The resulting expression is a production of the unitary color matrix and an exponential. This procedure is illustrated in Fig.1.

Inserting this expression into the matrix element \mathcal{M}_N , one obtains,

$$\begin{aligned} \mathcal{M}_N(x, \vec{k}_\perp) &= \int \frac{dr^- d^2 r_\perp}{(2\pi)^3} e^{ixP^+ r^- - i\vec{k}_\perp \cdot \vec{r}_\perp} \langle N | \bar{\psi}(y^-, y_\perp) \bar{U}^{[+]} \psi(r^- + y^-, r_\perp + y_\perp) | N \rangle \\ &\times \exp \left\{ -C_F \Theta(r_\perp^2) \int_{R^-+y^-}^{\infty} d\zeta^- \lambda_A(\zeta^-) \right\}. \end{aligned} \quad (7)$$

Here, the gauge link $\bar{U}^{[+]}$ is a short one and defined as,

$$\bar{U}^{[+]} = \mathcal{P} e^{-ig \int_{y^-}^{R^-+y^-} d\zeta^- A^+(\zeta^-, y_\perp)} \mathcal{P} e^{-ig \int_{R^-+y^-}^{r^-+y^-} d\zeta^- A^+(\zeta^-, r_\perp + y_\perp)}. \quad (8)$$

which consists of two short Wilson lines connected in color space at point $R^- + y^-$. Apparently, the density of the color sources outside a nucleon is zero: $\int_{R^-+y^-}^{\infty} d\zeta^- \lambda_A(\zeta^-) = 0$. Such vanishing contribution from gauge link outside a nucleon has also been clearly seen in the lattice calculation [42]. As a result, the exponential factor in the Eq.7 becomes unity. The TMD correlator is reduced to,

$$\begin{aligned} \mathcal{M}_N(x, \vec{k}_\perp) &= \int \frac{dr^- d^2 r_\perp}{(2\pi)^3} e^{ixP^+ r^- - i\vec{k}_\perp \cdot \vec{r}_\perp} \langle N | \bar{\psi}(0^-, 0_\perp) \bar{U}^{[+]} \psi(r^-, r_\perp) | N \rangle \\ &= \frac{1}{2} f_{1,DIS}(x, k_\perp) \not{p} + \frac{1}{2k_\perp} h_{1,DIS}^\perp(x, k_\perp) \sigma^{\mu\nu} k_\mu p_\nu, \end{aligned} \quad (9)$$

where we have shifted the coordinate y to zero using translation invariance.

Note that the above derivation applies to both nuclear and nucleon targets and that all results have the same form. The only difference is that for a large nucleus target, the struck nucleon is surrounded by cold nuclear matter, such that the density of color sources outside the struck nucleon is no longer zero.

$$\begin{aligned} \mathcal{M}_A(x, \vec{k}_\perp) &= \int \frac{dr^- d^2 r_\perp}{(2\pi)^3} e^{ixP^+ r^- - i\vec{k}_\perp \cdot \vec{r}_\perp} \langle A | \bar{\psi}(y^-, y_\perp) \bar{U}^{[+]} \psi(r^- + y^-, r_\perp + y_\perp) | A \rangle \\ &\quad \times \exp \left\{ -C_F \Theta(r_\perp^2) \int_{R^-+y^-}^{\infty} d\zeta^- \lambda_A(\zeta^-) \right\} \\ &= \frac{1}{2} \mathbf{f}_{1,DIS}(x, k_\perp) \not{p} + \frac{1}{2k_\perp} \mathbf{h}_{1,DIS}^\perp(x, k_\perp) \sigma^{\mu\nu} k_\mu p_\nu, \end{aligned} \quad (10)$$

where $\mathbf{f}_{1,DIS}$ and $\mathbf{h}_{1,DIS}^\perp$ denote the unpolarized quark and quark Boer-Mulders TMD distributions inside a large nucleus respectively. To proceed further, we make two assumptions:

1) we neglect the correlation between different nucleons and assume the large nucleus as a weakly bound,

$$\langle A | \bar{\psi}(y^-, y_\perp) \bar{U}^{[+]} \psi(r^- + y^-, r_\perp + y_\perp) | A \rangle = \langle N | \bar{\psi}(0^-, 0_\perp) \bar{U}^{[+]} \psi(r^-, r_\perp) | N \rangle \int dy^- d^2 y_\perp \rho_N^A(y), \quad (11)$$

where $|N\rangle$ is understood as the nucleon state averaged over protons and neutrons inside a large nucleus, and $\rho_N^A(y)$ is the spatial nucleon density normalized to the atomic number \mathcal{A} ;

2) we further describe the large nucleus as a homogenous system of nucleons and color sources,

$$\rho_N^A(y) = \rho_N^A(0), \quad \lambda_A(\zeta^-) = \lambda_A(0^-). \quad (12)$$

Implementing these two approximations, one has,

$$\begin{aligned} \mathcal{M}_A(x, \vec{k}_\perp) &= \int \frac{dr^- d^2 r_\perp}{(2\pi)^3} e^{ixP^+ r^- - i\vec{k}_\perp \cdot \vec{r}_\perp} \langle N | \bar{\psi}(0^-, 0_\perp) \bar{U}^{[+]} \psi(r^-, r_\perp) | N \rangle \\ &\quad \times \int dy^- d^2 y_\perp \rho_N^A(y^-) \exp \left\{ -C_F \Theta(r_\perp^2) \int_{R^-+y^-}^{\infty} d\zeta^- \lambda_A(\zeta^-) \right\} \\ &\approx \mathcal{A} \int \frac{dr^- d^2 r_\perp}{(2\pi)^3} e^{ixP^+ r^- - i\vec{k}_\perp \cdot \vec{r}_\perp} \langle N | \bar{\psi}(0^-, 0_\perp) \bar{U}^{[+]} \psi(r^-, r_\perp) | N \rangle \frac{1 - e^{-\frac{r_\perp^2 Q_{s,q}^2}{4}}}{r_\perp^2 Q_{s,q}^2 / 4} \end{aligned} \quad (13)$$

In the second step of the above equation, the approximation $\int_{R^-+y^-}^{\infty} d\zeta^- \lambda_A(\zeta^-) \approx \int_{y^-}^{\infty} d\zeta^- \lambda_A(\zeta^-)$ valid for a large nucleus target has been used. The quark saturation momentum $Q_{s,q}$ is given by $Q_{s,q}^2 = \alpha_s C_F \ln \frac{1}{r_\perp^2 \Lambda_{QCD}^2} \int_{-\infty}^{\infty} d\zeta^- \lambda_A(\zeta^-)$.

Eq.13 can be reexpressed in momentum space as,

$$\mathcal{M}_A(x, \vec{k}_\perp) = \mathcal{A} \int d^2 l_\perp \mathcal{M}_N(x, \vec{l}_\perp) \mathcal{F}_{DIS}(|\vec{k}_\perp - \vec{l}_\perp|). \quad (14)$$

Here $\mathcal{F}_{DIS}(|\vec{k}_\perp - \vec{l}_\perp|)$ is given by,

$$\mathcal{F}_{DIS}(|\vec{k}_\perp - \vec{l}_\perp|) = \int \frac{d^2 r_\perp}{(2\pi)^2} e^{-i(\vec{k}_\perp - \vec{l}_\perp) \cdot \vec{r}_\perp} 4 \frac{1 - e^{-\frac{r_\perp^2 Q_{s,q}^2}{4}}}{r_\perp^2 Q_{s,q}^2}, \quad (15)$$

and is normalized to 1: $\int d^2 l_\perp \mathcal{F}_{DIS}(l_\perp) = 1$. When $Q_{s,q}^2$ is small, the fact that $\mathcal{F}_{DIS}(|\vec{k}_\perp - \vec{l}_\perp|) \simeq \delta^2(\vec{k}_\perp - \vec{l}_\perp)$ allows us to recover the usual nucleon TMDs. Inserting the decomposition of the matrix correlator into Eq.14, it is easy to derive that,

$$\mathbf{f}_{1,DIS}(x, k_\perp) = \mathcal{A} \int d^2 l_\perp f_{1,DIS}(x, l_\perp) \mathcal{F}_{DIS}(|\vec{k}_\perp - \vec{l}_\perp|) \quad (16)$$

$$\mathbf{h}_{1,DIS}^\perp(x, k_\perp) = \mathcal{A} \int d^2 l_\perp (\hat{k}_\perp \cdot \hat{l}_\perp) h_{1,DIS}^\perp(x, l_\perp) \mathcal{F}_{DIS}(|\vec{k}_\perp - \vec{l}_\perp|). \quad (17)$$

The unit vectors \hat{k}_\perp and \hat{l}_\perp are defined as $\hat{k}_\perp \equiv \vec{k}_\perp/k_\perp$ and $\hat{l}_\perp \equiv \vec{l}_\perp/l_\perp$, respectively. From these relations between nucleon TMDs and nuclear TMDs, one finds,

$$\int d^2 k_\perp \mathbf{f}_{1,DIS}(x, k_\perp) = \mathcal{A} \int d^2 l_\perp f_{1,DIS}(x, l_\perp) = \mathcal{A} f_1(x) \quad (18)$$

$$\int d^2 k_\perp k_\perp^2 \mathbf{f}_{1,DIS}(x, k_\perp) = \mathcal{A} \int d^2 l_\perp l_\perp^2 f_{1,DIS}(x, l_\perp) + \frac{1}{2} Q_{s,q}^2 \mathcal{A} f_1(x) \quad (19)$$

$$\int d^2 k_\perp k_\perp \mathbf{h}_{1,DIS}^\perp(x, k_\perp) = \mathcal{A} \int d^2 l_\perp l_\perp h_{1,DIS}^\perp(x, l_\perp) = -2\pi M_N \mathcal{A} T_F^{(\sigma)}(x, x). \quad (20)$$

$f_1(x)$ is the normal integrated unpolarized quark distribution of a nucleon, while $T_F^{(\sigma)}(x, x)$ (convention used in Refs. [37, 38]) is the twist-3 quark gluon correlation function inside an unpolarized nucleon. In the last step of Eq.20, we used the well known relation between the moment of the Boer-Mulders function and $T_F^{(\sigma)}(x, x)$ [43]. It turns out that this relation is not affected by the cold nuclear medium. Moreover, for the approximations made in this paper, the unpolarized quarks inside a large nucleus are re-distributed in transverse momentum space while the total probability to find a quark carrying a certain longitudinal momentum fraction x remains unchanged. To be more specific, the quark transverse momentum distribution becomes broader and the transverse momentum broadening squared is $Q_{s,q}^2/2$.

In the semi-hard region where k_\perp^2 is of the order $Q_{s,q}^2$, Eq.16 and Eq.17 can be simplified by dropping the terms suppressed by powers $\langle l_\perp^2 \rangle / Q_{s,q}^2$ where $\langle l_\perp^2 \rangle$ is the average squared parton intrinsic transverse momentum inside a nucleon,

$$\mathbf{f}_{1,DIS}(x, k_\perp) \simeq \mathcal{A} f_1(x) \mathcal{F}_{DIS}(k_\perp) \quad (21)$$

$$\mathbf{h}_{1,DIS}^\perp(x, k_\perp) \simeq \mathcal{A} 2\pi M_N T_F^{(\sigma)}(x, x) \frac{1}{2} \frac{\partial \mathcal{F}_{DIS}(k_\perp)}{\partial k_\perp}, \quad (22)$$

which is the main result of this section. We believe that the main feature of multiple scattering in the cold nuclear matter has been captured in the above equations though various approximations were made in deriving them.

We conclude this subsection by emphasizing again the important point that the derivation presented above is only valid for nuclear TMDs at intermediate x or large x . In our calculation, it was critical to assume that the hard scattering takes place locally inside a nucleon, i.e., $r^- \leq R^-$. This is in sharp contrast to the dipole model where the quark antiquark pair coherently interacts with the whole nucleus.

2.2 The Drell-Yan process in pA collisions

We now turn to k_\perp broadening in Drell-Yan process. In a widely used hybrid approach (for a review, see [44]), one utilizes ordinary integrated parton distributions for the dilute projectile proton, while the transverse momentum carried by a parton coming from a nucleus is left unintegrated. We adopted the same strategy when dealing with pA collisions throughout this paper. As a consequence, at lowest order, the obtained transverse momentum spectrum of the produced virtual photon is directly related to the k_\perp^2 moment of the nuclear quark TMDs.

Quark TMDs appear in Drell-Yan differential cross sections contain a past-pointing gauge link,

$$U^{[-]} = \mathcal{P} e^{-ig \int_{y^-}^{-\infty} d\zeta^- A^+(\zeta^-, y_\perp)} \mathcal{P} e^{-ig \int_{-\infty}^{r^-+y^-} d\zeta^- A^+(\zeta^-, r_\perp+y_\perp)}. \quad (23)$$

Following the procedure outlined in the previous sub-section, one obtains the same relations between nucleon quark TMDs and nuclear quark TMDs,

$$\mathbf{f}_{1,DY}(x, k_\perp) = \mathcal{A} \int d^2 l_\perp f_{1,DY}(x, l_\perp) \mathcal{F}_{DY}(|\vec{k}_\perp - \vec{l}_\perp|) \quad (24)$$

$$\mathbf{h}_{1,DY}^\perp(x, k_\perp) = \mathcal{A} \int d^2 l_\perp (\hat{k}_\perp \cdot \hat{l}_\perp) h_{1,DY}^\perp(x, l_\perp) \mathcal{F}_{DY}(|\vec{k}_\perp - \vec{l}_\perp|), \quad (25)$$

with

$$\mathcal{F}_{DY}(|\vec{k}_\perp - \vec{l}_\perp|) = \mathcal{F}_{DIS}(|\vec{k}_\perp - \vec{l}_\perp|). \quad (26)$$

Similarly, a shorter past-pointing gauge link emerges in the matrix element definition for $f_{1,DY}(x, l_\perp)$ and $h_{1,DY}^\perp(x, l_\perp)$,

$$\bar{U}^{[-]} = \mathcal{P} e^{-ig \int_0^{-R^-} d\zeta^- A^+(\zeta^-, 0_\perp)} \mathcal{P} e^{-ig \int_{-R^-}^{r^-} d\zeta^- A^+(\zeta^-, r_\perp)}. \quad (27)$$

In the above formula, the coordinate y has again been shifted to zero by translation invariance. With this shorter gauge link, using time reversal and parity invariance, one may readily deduce,

$$f_{1,DY}(x, l_\perp) = f_{1,DIS}(x, l_\perp) \quad h_{1,DY}^\perp(x, l_\perp) = -h_{1,DIS}^\perp(x, l_\perp), \quad (28)$$

and therefore,

$$\mathbf{f}_{1,DY}(x, l_\perp) = \mathbf{f}_{1,DIS}(x, l_\perp) \quad \mathbf{h}_{1,DY}^\perp(x, l_\perp) = -\mathbf{h}_{1,DIS}^\perp(x, l_\perp). \quad (29)$$

We notice that the unique universality property of the T-odd distribution \mathbf{h}_1^\perp [45, 46] is preserved under our manipulation of gauge links. In the end, we would like to mention that the transverse momentum broadening for virtual photon produced in pA collisions is also parameterized by $Q_{s,q}^2/2$.

2.3 Heavy quark pair production in eA collisions

We study the nuclear broadening of heavy quark-antiquark pair momentum imbalance in eA collisions. Heavy quark production in eA collisions is initiated by the gluon channel,

$$\gamma^* + g \rightarrow Q + \bar{Q}. \quad (30)$$

The transverse momentum imbalance of a quark-antiquark pair is defined as

$$\vec{k}_\perp = \vec{p}_{1\perp} + \vec{p}_{2\perp} \quad (31)$$

where $\vec{p}_{1\perp}$ and $\vec{p}_{2\perp}$ are the transverse momenta of produced quark and antiquark, respectively. In TMD factorization and at leading order, \vec{k}_\perp is identical to the transverse momentum carried by the incoming gluon simply because of momentum conservation. The matrix element definition for nuclear gluon TMDs in SIDIS is given in [47, 48],

$$\begin{aligned}\mathcal{M}_A^{ij}(x, \vec{k}_\perp) &= \int \frac{dr^- d^2 r_\perp}{(2\pi)^3 P^+} e^{ixP^+ r^- - i\vec{k}_\perp \cdot \vec{r}_\perp} \langle A | F^{+i}(y^-, y_\perp) \tilde{U}^{[+]} L_y F^{+j}(r^- + y^-, r_\perp + y_\perp) | A \rangle \\ &= \frac{\delta_\perp^{ij}}{2} x \mathbf{G}_{DIS}(x, k_\perp) + \left(\hat{k}_\perp^i \hat{k}_\perp^j - \frac{1}{2} \delta_\perp^{ij} \right) x \mathbf{h}_{1,DIS}^{\perp g}(x, k_\perp),\end{aligned}\quad (32)$$

where $\tilde{U}^{[+]}$ is the future pointing gauge link in the adjoint representation. \mathbf{G}_{DIS} and $\mathbf{h}_{1,DIS}^{\perp g}$ stand for the unpolarized gluon TMD and linearly polarized gluon TMD respectively. $\mathbf{h}_{1,DIS}^{\perp g}$ is the only polarization dependent gluon TMD for an unpolarized nucleon/nucleus, and therefore may be considered as the counterpart of the quark Boer-Mulders function. However, in contrast to the later, $\mathbf{h}_{1,DIS}^{\perp g}$ is a time-reversal even distribution, implying $\mathbf{h}_{1,DIS}^{\perp g} = \mathbf{h}_{1,DY}^{\perp g}$. The linearly polarized gluon distribution inside a large nucleus recently attracted a lot of attentions. $\mathbf{h}^{\perp g}$ in the saturation regime was first derived using the MV model in [29]. Its rapidity evolution was also investigated [49]. Many processes in which $\mathbf{h}^{\perp g}$ can be probed have been proposed [29, 30, 49–51].

It is straightforward to extend our analysis for nuclear quark TMDs to gluon TMDs. One thus obtains,

$$\mathbf{G}_{DIS}(x, k_\perp) = \mathcal{A} \int d^2 l_\perp G_{DIS}(x, l_\perp) \mathcal{F}_{DIS}^g(|\vec{k}_\perp - \vec{l}_\perp|) \quad (33)$$

$$\mathbf{h}_{1,DIS}^{\perp g}(x, k_\perp) = \mathcal{A} \int d^2 l_\perp \left[2(\hat{k}_\perp \cdot \hat{l}_\perp)^2 - 1 \right] h_{1,DIS}^{\perp g}(x, l_\perp) \mathcal{F}_{DIS}^g(|\vec{k}_\perp - \vec{l}_\perp|). \quad (34)$$

G_{DIS} and $h_{1,DIS}^{\perp g}$ are corresponding gluon distributions in a nucleon. $\mathcal{F}_{DIS}^g(|\vec{k}_\perp - \vec{l}_\perp|)$ is given by,

$$\mathcal{F}_{DIS}^g(|\vec{k}_\perp - \vec{l}_\perp|) = \int \frac{d^2 r_\perp}{(2\pi)^2} e^{-i(\vec{k}_\perp - \vec{l}_\perp) \cdot \vec{r}_\perp} 4 \frac{1 - e^{-\frac{r_\perp^2 Q_s^2}{4}}}{r_\perp^2 Q_s^2}, \quad (35)$$

where $Q_s^2 = \alpha_s N_c \ln \frac{1}{r_\perp^2 \Lambda_{QCD}^2} \int_{-\infty}^{\infty} d\zeta^- \lambda_A(\zeta^-)$ is the gluon saturation momentum. With these relations, it is easy to further verify that,

$$\int d^2 k_\perp k_\perp^2 \mathbf{G}_{DIS}(x, k_\perp) = \mathcal{A} \int d^2 l_\perp l_\perp^2 G_{DIS}(x, l_\perp) + \frac{1}{2} Q_s^2 \mathcal{A} G_{DIS}(x) \quad (36)$$

$$\int d^2 k_\perp k_\perp^2 \mathbf{h}_{1,DIS}^{\perp g}(x, k_\perp) = \mathcal{A} \int d^2 l_\perp l_\perp^2 h_{1,DIS}^{\perp g}(x, l_\perp). \quad (37)$$

Correspondingly, the quark antiquark momentum imbalance in eA collisions is again of order $Q_s^2/2$.

3 Nuclear TMDs in photon-jet and heavy quark pair production in pA collisions

When both initial and final state interactions are present in a hard scattering, a more complicated structure of gauge links different from a simple past-pointing or future-pointing ones will appear. This results in the process dependent nuclear k_\perp broadening.

$$\begin{aligned}
& \text{Diagram: } (r^-, r_\perp) \xrightarrow{\leftarrow} (\infty, r_\perp) \\
& \text{Diagram: } (0^-, 0_\perp) \xrightarrow{\leftarrow} (\infty, 0_\perp) \\
= & \text{Diagram: } (0^-, 0_\perp) \xrightarrow{\leftarrow} (R^-, 0_\perp) \xrightarrow{\leftarrow} (R^-, r_\perp) \xrightarrow{\leftarrow} (r^-, r_\perp) \\
& \times \exp\left\{-N_c\Theta(r_\perp^2) \int_{R^-}^\infty d\zeta^- \lambda_A(\zeta^-)\right\} + \text{Diagram: } (0^-, 0_\perp) \xrightarrow{\leftarrow} (R^-, 0_\perp) \xrightarrow{\leftarrow} (r^-, r_\perp) \xrightarrow{\leftarrow} (R^-, r_\perp) \\
& \times \frac{1}{N_c} \left[1 - \exp\left\{-N_c\Theta(r_\perp^2) \int_{R^-}^\infty d\zeta^- \lambda_A(\zeta^-)\right\}\right]
\end{aligned}$$

Figure 2: The gauge link $U^{[+]}U^{[+]\dagger}$ is reduced to two short ones with different color structures by evaluating part of the gauge link stretching from R^- to ∞ in the MV model, where R^- is the radius of a nucleon.

3.1 Nuclear TMDs in photon-jet production

We first study the nuclear enhancement of the transverse momentum imbalance for photon-jet production in pA collisions,

$$p(P') + A(P) \rightarrow \gamma(p_1) + \text{Jet}(p_2) + X, \quad (38)$$

where P' and P are the momenta of incoming proton and nucleus(per nucleon), and p_1, p_2 are the momenta of the produced photon and jet respectively. The transverse momentum imbalance \vec{q}_\perp is defined as: $\vec{q}_\perp = \vec{p}_{1\perp} + \vec{p}_{2\perp}$.

For the $q\bar{q} \rightarrow \gamma g$ channel, the corresponding gauge link is built up by both initial state and final state interactions. The resulting nuclear quark TMDs are give by [25],

$$\begin{aligned}
\mathcal{M}_A(x, \vec{k}_\perp) &= \int \frac{dr^- d^2 r_\perp}{(2\pi)^3} e^{ixP^+ r^- - i\vec{k}_\perp \cdot \vec{r}_\perp} \\
&\times \langle A | \bar{\psi}(y^-, y_\perp) \left\{ \frac{9}{8N_c} U^{[+]} \text{Tr}_c[U^{\square\dagger}] - \frac{1}{8} U^{[-]} \right\} \psi(r^- + y^-, r_\perp + y_\perp) | A \rangle \\
&= \frac{1}{2} \mathbf{f}_{1, q\bar{q} \rightarrow \gamma g}(x, k_\perp) \not{p} + \frac{1}{2k_\perp} \mathbf{h}_{1, q\bar{q} \rightarrow \gamma g}^\perp(x, k_\perp) \sigma^{\mu\nu} k_\mu p_\nu, \quad (39)
\end{aligned}$$

where $U^{\square} = U^{[+]}U^{[-]\dagger} = U^{[-]\dagger}U^{[+]}$ emerges as a Wilson loop. The technique for evaluating multiple point correlation functions in the MV model has been systematically developed in Ref. [52]. The main strategy is to repeatedly use the Fierz identity $t_{ij}^a t_{kl}^a = \frac{1}{2} \delta_{il} \delta_{jk} - \frac{1}{2N_c} \delta_{ij} \delta_{kl}$ in order to resolve the color structure when gluon links connect different gauge links. By closely following the method presented in [52], we compute part of the gauge link $U^{[+]}U^{[+]\dagger}$ in the MV model,

$$\begin{aligned}
& \left\langle \left[\mathcal{P} e^{-ig \int_{y^-+R^-}^\infty d\zeta^- A^+(\zeta^-, y_\perp)} \mathcal{P} e^{-ig \int_\infty^{y^-+R^-} d\zeta^- A^+(r_\perp + y_\perp, \zeta^-)} \right]_{ij} \right. \\
& \quad \times \left. \left[\mathcal{P} e^{-ig \int_{y^-+R^-}^\infty d\zeta^- A^+(\zeta^-, y_\perp)} \mathcal{P} e^{-ig \int_\infty^{y^-+R^-} d\zeta^- A^+(r_\perp + y_\perp, \zeta^-)} \right]_{lm}^\dagger \right\rangle \\
&= \frac{1}{N_c} \left[1 - e^{-N_c\Theta(r_\perp^2) \int_{R^-+y^-}^\infty d\zeta^- \lambda_A(\zeta^-)} \right] \delta_{im} \delta_{jl} + e^{-N_c\Theta(r_\perp^2) \int_{R^-+y^-}^\infty d\zeta^- \lambda_A(\zeta^-)} \delta_{ij} \delta_{lm}, \quad (40)
\end{aligned}$$

where i, j, l and m are color indices. It is worthwhile to mention that two different topologies show up as illustrated in Fig.2. The gauge links $U^{[-]}$ and $U^{[+]}$ have also been calculated in the previous

section. Inserting these results into Eq.39, one obtains,

$$\begin{aligned}
\mathcal{M}_A(x, \vec{k}_\perp) &= \int \frac{dr^- d^2 r_\perp}{(2\pi)^3} e^{ixP^+ r^- - i\vec{k}_\perp \cdot \vec{r}_\perp} \int dy^- d^2 y_\perp \rho_N^A(y^-) \\
&\times \left\{ \langle N | \bar{\psi}(0^-, 0_\perp) \frac{9}{8} \bar{U}^{[+]} \frac{\text{Tr}_c[\bar{U}^{[\square]\dagger}]}{N_c} \psi(r^-, r_\perp) | N \rangle e^{-\Theta(r_\perp^2)} \left[C_F \int_{-\infty}^{y^- - R^-} d\zeta^- \lambda_A(\zeta^-) + N_c \int_{y^- + R^-}^{\infty} d\zeta^- \lambda_A(\zeta^-) \right] \right. \\
&+ \langle N | \bar{\psi}(0^-, 0_\perp) \frac{1}{8} \bar{U}^{[-]} \psi(r^-, r_\perp) | N \rangle e^{-C_F \Theta(r_\perp^2)} \int_{-\infty}^{y^- - R^-} d\zeta^- \lambda_A(\zeta^-) \left[1 - e^{-N_c \Theta(r_\perp^2)} \int_{y^- + R^-}^{\infty} d\zeta^- \lambda_A(\zeta^-) \right] \\
&\left. - \langle N | \bar{\psi}(0^-, 0_\perp) \frac{1}{8} \bar{U}^{[-]} \psi(r^-, r_\perp) | N \rangle e^{-C_F \Theta(r_\perp^2)} \int_{-\infty}^{y^- - R^-} d\zeta^- \lambda_A(\zeta^-) \right\}. \quad (41)
\end{aligned}$$

The short Wilson loop appearing in the above equation consists of a short future-pointing and a short past-pointing gauge link: $\bar{U}^{[\square]} = \bar{U}^{[+]} \bar{U}^{[-]\dagger}$. By approximating the large nucleus as a homogenous system of color sources, we are able to carry out the integration over y^- and y_\perp . One then ends up with,

$$\begin{aligned}
\mathcal{M}_A(x, \vec{k}_\perp) &= \int \frac{dr^- d^2 r_\perp}{(2\pi)^3} e^{ixP^+ r^- - i\vec{k}_\perp \cdot \vec{r}_\perp} \\
&\times \mathcal{A} \langle N | \bar{\psi}(0^-, 0_\perp) \left\{ \frac{9}{8} \bar{U}^{[+]} \frac{\text{Tr}_c[\bar{U}^{[\square]\dagger}]}{N_c} - \frac{1}{8} \bar{U}^{[-]} \right\} \psi(r^-, r_\perp) | N \rangle \left[\frac{e^{-\frac{Q_s^2 r_\perp^2}{4}} - e^{-\frac{Q_{s,q}^2 r_\perp^2}{4}}}{(Q_{s,q}^2 - Q_s^2) r_\perp^2 / 4} \right], \quad (42)
\end{aligned}$$

where $Q_s^2 = \alpha_s N_c \ln \frac{1}{r_\perp^2 \Lambda_{QCD}^2} \int_{-\infty}^{\infty} d\zeta^- \lambda_A(\zeta^-)$ is the gluon saturation momentum. To arrive the above equation, we have made one further approximation, $\int_{-\infty}^{y^- - R^-} d\zeta^- \lambda_A(\zeta^-) + \int_{y^- + R^-}^{\infty} d\zeta^- \lambda_A(\zeta^-) \approx \int_{-\infty}^{\infty} d\zeta^- \lambda_A(\zeta^-)$, which is valid for a large nucleus. One can readily transform this expression to momentum space,

$$\mathbf{f}_{1,q\bar{q} \rightarrow \gamma g}(x, k_\perp) = \mathcal{A} \int d^2 l_\perp f_{1,q\bar{q} \rightarrow \gamma g}(x, l_\perp) \mathcal{F}_{q\bar{q} \rightarrow \gamma g}(|\vec{k}_\perp - \vec{l}_\perp|) \quad (43)$$

$$\mathbf{h}_{1,q\bar{q} \rightarrow \gamma g}^\perp(x, k_\perp) = \mathcal{A} \int d^2 l_\perp (\hat{k}_\perp \cdot \hat{l}_\perp) h_{1,q\bar{q} \rightarrow \gamma g}^\perp(x, l_\perp) \mathcal{F}_{q\bar{q} \rightarrow \gamma g}(|\vec{k}_\perp - \vec{l}_\perp|), \quad (44)$$

with $\mathcal{F}_{q\bar{q} \rightarrow \gamma g}(k_\perp)$ being given by,

$$\mathcal{F}_{q\bar{q} \rightarrow \gamma g}(|\vec{k}_\perp - \vec{l}_\perp|) = \int \frac{d^2 r_\perp}{(2\pi)^2} e^{-i(\vec{k}_\perp - \vec{l}_\perp) \cdot \vec{r}_\perp} \frac{e^{-\frac{Q_s^2 r_\perp^2}{4}} - e^{-\frac{Q_{s,q}^2 r_\perp^2}{4}}}{(Q_{s,q}^2 - Q_s^2) r_\perp^2 / 4}. \quad (45)$$

Correspondingly, the k_\perp moment of nuclear TMDs read,

$$\int d^2 k_\perp k_\perp^2 \mathbf{f}_{1,q\bar{q} \rightarrow \gamma g}(x, k_\perp) = \mathcal{A} \int d^2 l_\perp l_\perp^2 f_{1,q\bar{q} \rightarrow \gamma g}(x, l_\perp) + \left[\frac{1}{2} Q_{s,q}^2 + \frac{1}{2} Q_s^2 \right] \mathcal{A} f_1(x) \quad (46)$$

$$\int d^2 k_\perp k_\perp \mathbf{h}_{1,q\bar{q} \rightarrow \gamma g}^\perp(x, k_\perp) = \mathcal{A} \int d^2 l_\perp l_\perp h_{1,q\bar{q} \rightarrow \gamma g}^\perp(x, l_\perp) = -2\pi M_N \mathcal{A} \frac{N_c^2 + 1}{N_c^2 - 1} T_F^{(\sigma)}(x, x), \quad (47)$$

where the nontrivial color factor $(N_c^2 + 1)/(N_c^2 - 1)$ originates from the T-odd nature of the quark Boer-Mulders distribution. In the semihard region where the imbalance of the photon-jet produced

in pA collisions is of the order $Q_s \gg \Lambda_{QCD}$, after neglecting the terms suppressed by the power of Λ_{QCD}^2/Q_s^2 , we have,

$$\mathbf{f}_{1,q\bar{q}\rightarrow\gamma g}(x, k_\perp) \simeq \mathcal{A}f_1(x)\mathcal{F}_{q\bar{q}\rightarrow\gamma g}(k_\perp) \quad (48)$$

$$\mathbf{h}_{1,q\bar{q}\rightarrow\gamma g}^\perp(x, k_\perp) \simeq \mathcal{A}2\pi M_N \frac{N_c^2 + 1}{N_c^2 - 1} T_F^{(\sigma)}(x, x) \frac{1}{2} \frac{\partial \mathcal{F}_{q\bar{q}\rightarrow\gamma g}(k_\perp)}{\partial k_\perp}. \quad (49)$$

The nuclear quark Boer-Mulders function can manifest itself through $\cos 2\phi$ asymmetries as can be seen by convoluting with the function $T_F^{(\sigma)}$ from the proton side. Moreover, if the incoming proton is transversely polarized, the quark Boer-Mulders function can couple with the transversity distribution of the proton and give rise to the single transverse spin asymmetry(SSA). Such observable in pA collisions was also studied from a different points of view in the papers [53–56].

Photon-jet pair can also be produced through other three channels: $\bar{q}q \rightarrow \gamma g$, $qg \rightarrow \gamma q$ and $gq \rightarrow \gamma q$. The associated nuclear TMDs contain different gauge link structures in the different channels. By evaluating the gauge links in the MV model, it is straightforward to establish the relations between nucleon TMDs and nuclear TMDs in these processes. However, for simplicity, we only list the k_\perp momenta of the corresponding nuclear TMDs,

$$\int d^2k_\perp k_\perp^2 \bar{\mathbf{f}}_{1,\bar{q}q\rightarrow\gamma g}(x, k_\perp) = \mathcal{A} \int d^2l_\perp l_\perp^2 \bar{f}_{1,\bar{q}q\rightarrow\gamma g}(x, l_\perp) + \left[\frac{1}{2}Q_{s,q}^2 + \frac{1}{2}Q_s^2 \right] \mathcal{A}\bar{f}_1(x) \quad (50)$$

$$\int d^2k_\perp k_\perp^2 \mathbf{f}_{1,qg\rightarrow\gamma q}(x, k_\perp) = \mathcal{A} \int d^2l_\perp l_\perp^2 f_{1,qg\rightarrow\gamma q}(x, l_\perp) + \left[\frac{1}{2}Q_{s,q}^2 + \frac{1}{2}Q_s^2 \right] \mathcal{A}f_1(x) \quad (51)$$

$$\int d^2k_\perp k_\perp^2 \mathbf{G}_{gq\rightarrow\gamma q}(x, k_\perp) = \mathcal{A} \int d^2l_\perp l_\perp^2 G_{gq\rightarrow\gamma q}(x, l_\perp) + Q_{s,q}^2 \mathcal{A}G(x), \quad (52)$$

where $\bar{\mathbf{f}}_1$ denotes the anti-quark distribution.

The average squared transverse momentum imbalance is given by,

$$\langle q_\perp^2 \rangle = \left(\int d^2q_\perp q_\perp^2 \frac{d\sigma}{d\mathcal{P} \cdot \mathcal{S} \cdot d^2q_\perp} \right) / \frac{d\sigma}{d\mathcal{P} \cdot \mathcal{S}} \quad (53)$$

where $d\mathcal{P} \cdot \mathcal{S} = dy_1 dy_2 d^2p_\perp$ stands for the phase space with y_1, y_2 being the produced photon and jet rapidities respectively. The nuclear broadening of the photon-jet imbalance is defined as

$$\Delta \langle q_\perp^2 \rangle = \langle q_\perp^2 \rangle_{pA} - \langle q_\perp^2 \rangle_{pp}, \quad (54)$$

Putting all these together, within the TMD factorization framework the nuclear enhancement of the photon-jet squared transverse momentum imbalance is given by,

$$\Delta \langle q_\perp^2 \rangle = \Delta \langle k_\perp^2 \rangle = \frac{1}{2}Q_{s,q}^2 + \frac{1}{2}Q_s^2 - \frac{\left[\frac{1}{2}Q_s^2 - \frac{1}{2}Q_{s,q}^2 \right] \Sigma_a H_{gq\rightarrow\gamma q}^a}{\Sigma_a \left[H_{gq\rightarrow\gamma q}^a + H_{gq\rightarrow\gamma q}^a + H_{q\bar{q}\rightarrow\gamma g}^a + H_{q\bar{q}\rightarrow\gamma g}^a \right]}, \quad (55)$$

where a runs all quark flavors. The partonic hard scattering differential cross sections read [57],

$$H_{gq\rightarrow\gamma q}^a = e_q^2 \frac{1}{N_c} \left(-\frac{\hat{s}}{\hat{t}} - \frac{\hat{t}}{\hat{s}} \right) \mathbf{f}_1^a(x) G(x') \quad (56)$$

$$H_{gq\rightarrow\gamma q}^a = e_q^2 \frac{1}{N_c} \left(-\frac{\hat{s}}{\hat{u}} - \frac{\hat{u}}{\hat{s}} \right) \mathbf{G}(x) f_1^a(x') \quad (57)$$

$$H_{q\bar{q}\rightarrow\gamma g}^a = e_q^2 \frac{N_c^2 - 1}{N_c^2} \left(\frac{\hat{t}}{\hat{u}} + \frac{\hat{u}}{\hat{t}} \right) \mathbf{f}_1^a(x) \bar{f}_1^a(x') \quad (58)$$

$$H_{q\bar{q}\rightarrow\gamma g}^a = e_q^2 \frac{N_c^2 - 1}{N_c^2} \left(\frac{\hat{t}}{\hat{u}} + \frac{\hat{u}}{\hat{t}} \right) \bar{\mathbf{f}}_1^a(x) f_1^a(x') \quad (59)$$

Here, \hat{s} , \hat{u} and \hat{t} are the usual partonic Mandelstam variables. The collinear momentum fraction is fixed by the kinematical constraint,

$$x' = \frac{p_\perp}{\sqrt{s}}(e^{y_1} + e^{y_2}), \quad x'' = \frac{p_\perp}{\sqrt{s}}(e^{-y_1} + e^{-y_2}) \quad (60)$$

where $s = (P+P')^2$ is the center of mass energy squared. By noticing $Q_s^2 = \frac{C_A}{C_F} Q_{s,q}^2$, the nuclear broadening of the photon-jet imbalance varies from $1\frac{5}{8} Q_{s,q}^2$ to $Q_{s,q}^2$ depending on the specific kinematical variables.

3.2 k_\perp broadening in heavy quark pair production

Quark antiquark pair production in high energy pA collisions is dominated by the gluon initiated parton subprocess,

$$g_p(x_1 P') + g_A(x_2 P) \rightarrow Q(p_1) + \bar{Q}(p_2). \quad (61)$$

The nuclear enhancement of the quark pair transverse momentum imbalance $\vec{q}_\perp = \vec{p}_{1\perp} + \vec{p}_{2\perp}$ is directly sensitive to nuclear gluon TMD distributions. The color flow in this subprocess is more complicated than that for photon-jet production in pA collisions. The nuclear gluon TMDs associated with different Feynman diagrams contain different gauge link structures. Here we show two examples,

$$\mathcal{M}_A^a \propto \langle A | \text{Tr}_c \left[F_{+\perp} \left\{ \frac{9}{8} \frac{\text{Tr}_c[U^{\square\dagger}]}{N_c} U^{[-]\dagger} - \frac{1}{8} U^{[+]\dagger} \right\} F_{+\perp} U^{[+]} \right] | A \rangle \quad (62)$$

$$\mathcal{M}_A^e \propto \langle A | \text{Tr}_c \left[F_{+\perp} U^{[-]\dagger} F_{+\perp} U^{[+]} \right] \frac{\text{Tr}_c[U^{\square\dagger}]}{N_c} - \frac{1}{N_c} \text{Tr}_c \left[F_{+\perp} U^{\square\dagger} \right] \text{Tr}_c \left[F_{+\perp} U^{\square} \right] | A \rangle, \quad (63)$$

where gauge links appearing in \mathcal{M}_A^a and \mathcal{M}_A^e originate from initial/final state interactions in the Feynman diagrams Fig.3(a) and Fig.3(e), respectively. All other gauge links appearing in this hard scattering process are given in [25]. One can compute the transverse momentum spectrum of the gluon distribution associated with each Feynman diagram following a similar method as introduced in the previous subsections. With the derived nuclear gluon TMDs, we obtain,

$$\int d^2 k_\perp k_\perp^2 \mathbf{G}_{gg \rightarrow Q\bar{Q}}^a(x, k_\perp) = \mathcal{A} \int d^2 l_\perp l_\perp^2 G_{gg \rightarrow Q\bar{Q}}^a(x, l_\perp) + \left[1 - \frac{1}{2 N_c^2 - 1} \right] Q_s^2 \mathcal{A} G(x) \quad (64)$$

$$\int d^2 k_\perp k_\perp^2 \mathbf{G}_{gg \rightarrow Q\bar{Q}}^b(x, k_\perp) = \mathcal{A} \int d^2 l_\perp l_\perp^2 G_{gg \rightarrow Q\bar{Q}}^b(x, l_\perp) + \left[1 - \frac{1}{2 N_c^2 - 1} \right] Q_s^2 \mathcal{A} G(x) \quad (65)$$

$$\int d^2 k_\perp k_\perp^2 \mathbf{G}_{gg \rightarrow Q\bar{Q}}^c(x, k_\perp) = \mathcal{A} \int d^2 l_\perp l_\perp^2 G_{gg \rightarrow Q\bar{Q}}^c(x, l_\perp) + \frac{3}{2} Q_s^2 \mathcal{A} G(x) \quad (66)$$

$$\int d^2 k_\perp k_\perp^2 \mathbf{G}_{gg \rightarrow Q\bar{Q}}^d(x, k_\perp) = \mathcal{A} \int d^2 l_\perp l_\perp^2 G_{gg \rightarrow Q\bar{Q}}^d(x, l_\perp) + Q_s^2 \mathcal{A} G(x) \quad (67)$$

$$\int d^2 k_\perp k_\perp^2 \mathbf{G}_{gg \rightarrow Q\bar{Q}}^e(x, k_\perp) = \mathcal{A} \int d^2 l_\perp l_\perp^2 G_{gg \rightarrow Q\bar{Q}}^e(x, l_\perp) + Q_s^2 \mathcal{A} G(x) \quad (68)$$

$$\int d^2 k_\perp k_\perp^2 \mathbf{G}_{gg \rightarrow Q\bar{Q}}^f(x, k_\perp) = \mathcal{A} \int d^2 l_\perp l_\perp^2 G_{gg \rightarrow Q\bar{Q}}^f(x, l_\perp) + Q_s^2 \mathcal{A} G(x). \quad (69)$$

It is easy to verify that the hard coefficient computed from the Feynman diagram Fig.3(c) is suppressed by the factor of $1/N_c^2$ as compared to the contributions from other diagrams in the large N_c limit. Thus, we conclude that the nuclear k_\perp broadening for quark antiquark pair production in pA collisions is Q_s^2 in the large N_c limit.

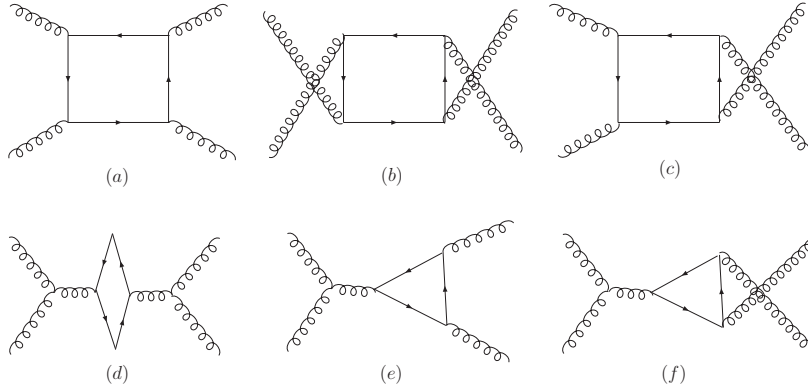


Figure 3: Feynman diagrams contributing to quark antiquark pair production.

4 Phenomenology applications

In this section, we discuss phenomenology applications of our results and compare our formalism with the higher twist collinear approach. We start from numerically evaluating nuclear k_{\perp} broadening for jet production in eA collisions. The analytical result for this observable takes a simple form,

$$\Delta < k_{\perp}^2 >_{\gamma^* q \rightarrow q} = Q_{s,q}^2/2. \quad (70)$$

However, in deriving the above result, we only took into account the contributions to the gauge link from color sources outside of the nucleon to which the struck parton belongs. To remedy this problem, the above equation should be slightly modified as follows,

$$\Delta < k_{\perp}^2 >_{\gamma^* q \rightarrow q} = \frac{\mathcal{A}^{1/3} - 1}{\mathcal{A}^{1/3}} Q_{s,q}^2/2, \quad (71)$$

where we adopt the parametrization for the saturation momentum used in the GBW model [58]: $Q_s^2 = \mathcal{A}^{1/3} Q_0^2 (x_0/x_g)^\lambda$ with $Q_0^2 = 1 \text{ GeV}^2$, $x_0 = 3 \cdot 10^{-4}$ and $\lambda \approx 0.3$. For a lead or gold targets, $\mathcal{A}^{1/3} - 1$ is approximately equal to 5.

The natural next step is to fix x_g . At first glance, gluons building up gauge links carry exactly zero longitudinal momentum due to the contour integration around the gluon pole $1/(x_g - i\epsilon)$ (for final state interactions). This pole arises when performing the calculation in the collinear approximation. However, if one keeps the gluon transverse momentum $k_{g\perp}$, the gluon pole in jet production in the SIDIS process will be modified to,

$$\frac{1}{x_g - k_{g\perp}^2/(2p \cdot q) - i\epsilon}, \quad (72)$$

where q is the virtual photon momentum. Within the leading logarithm accuracy, it is convenient to replace $k_{g\perp}^2$ in above formula by $\Delta < k_{\perp}^2 >$. Once x_g is fixed as $\Delta < k_{\perp}^2 > / (2p \cdot q)$, one obtains (for a lead or gold target),

$$\Delta < k_{\perp}^2 >_{\gamma^* q \rightarrow q} = \left[\frac{1}{2} \frac{C_F}{C_A} (\mathcal{A}^{1/3} - 1) Q_0^2 \right]^{1/(1+\lambda)} \left(s \frac{x_0}{1+x_B} \right)^{\lambda/(1+\lambda)} \approx 1.08 \left(s \frac{x_0}{1+x_B} \right)^{0.23} (Q_0^2)^{0.77}, \quad (73)$$

where $s = (p+q)^2$ and $x_B \equiv Q^2/2p \cdot q = Q^2/(s+Q^2)$ with $Q^2 = -q^2$ being the virtual photon virtuality. The above equation holds as long as x_B is of the order of 1 and $x_g \leq 0.01$ where the

MV model can apply. This implies that our formalism is invalid at relatively low energy [59]. Given $x_B = 0.2$ and $\sqrt{s} = 35\text{GeV}$ accessible at a future EIC, the nuclear k_\perp broadening for jet production in the SIDIS process gives $\Delta < k_\perp^2 >_{\gamma^*q \rightarrow q} \approx 0.82\text{GeV}^2$. For the Drell-Yan process one can fix the saturation scale in the same way. Unfortunately, we are not able to unambiguously determine the saturation scale for other processes.

Now we compare our result with that obtained from the higher twist collinear approach. As mentioned in the introduction, the process dependent k_\perp broadening effect was also investigated within the higher twist collinear factorization framework [33, 34] which can be applied in the intermediate or large x region. In this formalism, the effect of initial/final state multiple scattering generating k_\perp broadening is encoded in the collinear twist-4 quark-gluon correlation functions $T_{q,g/A}^{(I)}(x)$ and $T_{q,g/A}^{(F)}(x)$. These functions are parameterized as follows,

$$\frac{4\pi^2\alpha_s}{N_c}T_{q,g/A}^{(I)}(x) = \frac{4\pi^2\alpha_s}{N_c}T_{q,g/A}^{(F)}(x) = \xi^2(\mathcal{A}^{1/3} - 1)f_{q,g/A}(x), \quad (74)$$

where ξ^2 represents a characteristic scale of parton multiple scattering, and $f_{q,g/A}(x)$ is the standard leading-twist parton distribution function for quarks and gluons, respectively. If we identify the saturation scale as,

$$\frac{1}{2} \frac{Q_{s,q}^2}{C_F} = \frac{1}{2} \frac{Q_s^2}{C_A} = \xi^2 \mathcal{A}^{1/3}, \quad (75)$$

our analytical results for k_\perp broadening take the same form as those presented in [33, 34]. In [33, 34], ξ^2 is chosen to be 0.12GeV^2 . Provided that one evaluates the saturation scale using the same value $\xi^2 = 0.12\text{GeV}^2$, we have numerical result for jet k_\perp broadening in SIDIS $\Delta < k_\perp^2 >_{\gamma^*q \rightarrow q} = 0.8\text{GeV}^2$, which is very close to that calculated with the GBW parametrization. We would also get the identical numerical results for all other processes using Eq.75.

Apart from the process dependent unpolarized nuclear TMDs, the process dependent nuclear quark Boder-Mulders function is also studied in this paper. Below we discuss the corresponding phenomenological implications for the polarized cases. In both SIDIS and DY in pA collisions, the nuclear quark Boer-Mulders function can give rise to $\cos 2\phi$ azimuthal asymmetries by coupling with the Collins fragmentation function and the anti-quark Boer-Mulders function from the proton side [60], respectively. According to our calculation, in the semi-hard region, the transverse momentum dependence of the asymmetry is unambiguously determined by the ratio,

$$\langle \cos 2\phi \rangle(k_\perp) \propto \frac{\partial \mathcal{F}_{DIS}(k_\perp)}{\partial k_\perp} / \mathcal{F}_{DIS}(k_\perp).$$

Such observables can in principle be measured in unpolarized eA collisions at EIC and unpolarized pA collisions at RHIC. We leave detailed phenomenological studies for a future work.

5 Summary

We have established relations between nuclear TMDs and the corresponding nucleon ones by computing contributions from the process dependent gauge links in the MV model. In particular, in the semi-hard region where quark transverse momenta are of the order of the saturation scale, unpolarized nuclear TMDs are determined by the process dependent small x gluon distributions, while nuclear quark Boer-Mulders distributions are expressed as products of $T_F^{(\sigma)}(x, x)$ and the differential

of the same gluon distributions with respect to gluon transverse momentum. We stress again that the formalism developed in this paper applies only for nuclear TMDs at intermediate or large x .

Two phenomenological applications of our work are nuclear k_{\perp} broadening and the k_{\perp} dependence of the asymmetries generated by the quark Boer-Mulders function in eA and pA collisions. To be more specific, we calculated nuclear k_{\perp} broadening for jet and di-jet production in eA collisions, and the nuclear enhancement of the transverse momentum imbalance for Drell-Yan lepton pair production, photon-jet production, and quark antiquark pair production in pA collisions. To investigate how the quark Boer-Mulders function are affected by the surrounding cold nuclear matter, we also proposed to measure $\cos 2\phi$ azimuthal asymmetries in SIDIS off a large nucleus and Drell-Yan pairs in pA collisions. It will be interesting to test our predications at RHIC and the planned EIC.

Acknowledgments: This work has been supported by BMBF (OR 06RY9191 and 05P12WRFTE).

References

- [1] G. T. Bodwin, S. J. Brodsky and G. P. Lepage, Phys. Rev. Lett. **47**, 1799 (1981); Phys. Rev. D **39**, 3287 (1989).
- [2] M. Luo, J. -w. Qiu, G. F. Sterman, Phys. Lett. **B279**, 377-383 (1992); Phys. Rev. **D49**, 4493-4502 (1994); Phys. Rev. **D50**, 1951-1971 (1994).
- [3] R. J. Fries, Phys. Rev. D **68**, 074013 (2003).
- [4] A. Majumder, B. Muller, Phys. Rev. **C77**, 054903 (2008).
- [5] J. Dolejsi, J. Hufner and B. Z. Kopeliovich, Phys. Lett. B **312**, 235 (1993) [hep-ph/9305238].
- [6] M. B. Johnson, B. Z. Kopeliovich and A. V. Tarasov, Phys. Rev. C **63**, 035203 (2001) [hep-ph/0006326].
- [7] R. Baier, Y. L. Dokshitzer, A. H. Mueller, S. Peigne and D. Schiff, Nucl. Phys. B **484**, 265 (1997).
- [8] B. Wu, JHEP **1110**, 029 (2011) [arXiv:1102.0388 [hep-ph]].
- [9] T. Liou, A. H. Mueller and B. Wu, arXiv:1304.7677 [hep-ph].
- [10] A. Dumitru and J. Jalilian-Marian, Phys. Lett. B **547**, 15 (2002) [hep-ph/0111357].
- [11] D. Kharzeev, Y. V. Kovchegov and K. Tuchin, Phys. Rev. D **68**, 094013 (2003) [hep-ph/0307037].
- [12] M. Gyulassy, P. Levai and I. Vitev, Phys. Rev. D **66**, 014005 (2002) [nucl-th/0201078].
- [13] Z. T. Liang, X. N. Wang and J. Zhou, Phys. Rev. D **77**, 125010 (2008)
- [14] A. Idilbi and A. Majumder, Phys. Rev. D **80**, 054022 (2009) [arXiv:0808.1087 [hep-ph]].
- [15] F. D’Eramo, H. Liu and K. Rajagopal, Phys. Rev. D **84**, 065015 (2011).
- [16] G. Ovanesyan and I. Vitev, JHEP **1106**, 080 (2011) [arXiv:1103.1074 [hep-ph]].
- [17] M. Benzke, N. Brambilla, M. A. Escobedo and A. Vairo, JHEP **1302**, 129 (2013) [arXiv:1208.4253 [hep-ph]].

- [18] J. Casalderrey-Solana and X. -N. Wang, Phys. Rev. C **77**, 024902 (2008) [arXiv:0705.1352 [hep-ph]].
- [19] A. H. Mueller and S. Munier, Nucl. Phys. A **893**, 43 (2012) [arXiv:1206.1333 [hep-ph]].
- [20] J. C. Collins and D. E. Soper, Nucl. Phys. B **193**, 381 (1981) [Erratum-ibid. B **213**, 545 (1983)]; Nucl. Phys. B **194**, 445 (1982).
- [21] X. D. Ji, J. P. Ma and F. Yuan, Phys. Rev. D **71**, 034005 (2005).
- [22] J. -H. Gao, Z. -t. Liang, X. -N. Wang, Phys. Rev. **C81**, 065211 (2010).
- [23] Y. -k. Song, J. -h. Gao, Z. -t. Liang, X. -N. Wang, Phys. Rev. **D83**, 054010 (2011).
- [24] J. -H. Gao, A. Schafer and J. Zhou, Phys. Rev. D **85**, 074027 (2012) [arXiv:1111.1633 [hep-ph]].
- [25] C. J. Bomhof, P. J. Mulders and F. Pijlman, Phys. Lett. B **596**, 277 (2004) [hep-ph/0406099]; Eur. Phys. J. C **47**, 147 (2006) [arXiv:hep-ph/0601171].
- [26] B. -W. Xiao and F. Yuan, Phys. Rev. Lett. **105**, 062001 (2010) [arXiv:1003.0482 [hep-ph]]; Phys. Rev. D **82**, 114009 (2010) [arXiv:1008.4432 [hep-ph]].
- [27] F. Dominguez, B. W. Xiao and F. Yuan, Phys. Rev. Lett. **106**, 022301 (2011) [arXiv:1009.2141 [hep-ph]].
- [28] F. Dominguez, C. Marquet, B. W. Xiao and F. Yuan, Phys. Rev. D **83**, 105005 (2011) [arXiv:1101.0715 [hep-ph]].
- [29] A. Metz and J. Zhou, Phys. Rev. D **84**, 051503 (2011) [arXiv:1105.1991 [hep-ph]].
- [30] E. Akcakaya, A. Schafer and J. Zhou, Phys. Rev. D **87**, 054010 (2013) [arXiv:1208.4965 [hep-ph]].
- [31] T. C. Rogers and P. J. Mulders, Phys. Rev. D **81**, 094006 (2010) [arXiv:1001.2977 [hep-ph]].
- [32] Z. -B. Kang and J. -W. Qiu, Phys. Rev. D **77**, 114027 (2008) [arXiv:0802.2904 [hep-ph]]; Phys. Lett. B **721**, 277 (2013) [arXiv:1212.6541 [hep-ph]].
- [33] Z. -B. Kang, I. Vitev and H. Xing, Phys. Rev. D **85**, 054024 (2012) [arXiv:1112.6021 [hep-ph]].
- [34] H. Xing, Z. -B. Kang, I. Vitev and E. Wang, Phys. Rev. D **86**, 094010 (2012) [arXiv:1206.1826 [hep-ph]].
- [35] L. D. McLerran and R. Venugopalan, Phys. Rev. D **49**, 2233 (1994) [arXiv:hep-ph/9309289]; Phys. Rev. D **49**, 3352 (1994) [arXiv:hep-ph/9311205].
- [36] D. Boer, P. J. Mulders, Phys. Rev. **D57**, 5780-5786 (1998).
- [37] J. Zhou, F. Yuan and Z. -T. Liang, Phys. Rev. D **78**, 114008 (2008) [arXiv:0808.3629 [hep-ph]].
- [38] J. Zhou, F. Yuan and Z. -T. Liang, Phys. Rev. D **81**, 054008 (2010) [arXiv:0909.2238 [hep-ph]].
- [39] J. Zhou, F. Yuan, Z. -T. Liang, Phys. Lett. **B678**, 264-268 (2009).
- [40] X. D. Ji and F. Yuan, Phys. Lett. B **543**, 66 (2002). A. V. Belitsky, X. Ji and F. Yuan, Nucl. Phys. B **656**, 165 (2003).

- [41] E. Iancu, A. Leonidov and L. McLerran, arXiv:hep-ph/0202270.
- [42] B. U. Musch, P. Hagler, M. Engelhardt, J. W. Negele and A. Schafer, Phys. Rev. D **85**, 094510 (2012) [arXiv:1111.4249 [hep-lat]].
- [43] D. Boer, P. J. Mulders and F. Pijlman, Nucl. Phys. B **667**, 201 (2003) [hep-ph/0303034].
- [44] J. Jalilian-Marian and Y. V. Kovchegov, Prog. Part. Nucl. Phys. **56**, 104 (2006) [arXiv:hep-ph/0505052].
- [45] S. J. Brodsky, D. S. Hwang and I. Schmidt, Phys. Lett. B **530**, 99 (2002) [arXiv:hep-ph/0201296].
- [46] J. C. Collins, Phys. Lett. B **536**, 43 (2002) [arXiv:hep-ph/0204004].
- [47] P. J. Mulders and J. Rodrigues, Phys. Rev. D **63**, 094021 (2001) [arXiv:hep-ph/0009343].
- [48] M. Anselmino, M. Boglione, U. D'Alesio, E. Leader, S. Melis and F. Murgia, Phys. Rev. D **73**, 014020 (2006) [arXiv:hep-ph/0509035]. S. Meissner, A. Metz and K. Goeke, Phys. Rev. D **76**, 034002 (2007) [arXiv:hep-ph/0703176].
- [49] F. Dominguez, J. -W. Qiu, B. -W. Xiao and F. Yuan, Phys. Rev. D **85**, 045003 (2012) [arXiv:1109.6293 [hep-ph]].
- [50] A. Schafer and J. Zhou, Phys. Rev. D **85**, 114004 (2012) [arXiv:1203.1534 [hep-ph]].
- [51] T. Liou, Nucl. Phys. A **897**, 122 (2013) [arXiv:1206.6123 [hep-ph]].
- [52] J. P. Blaizot, F. Gelis and R. Venugopalan, Nucl. Phys. A **743**, 57 (2004) [hep-ph/0402257].
- [53] D. Boer and A. Dumitru, Phys. Lett. B **556**, 33 (2003) [hep-ph/0212260]. D. Boer, A. Dumitru and A. Hayashigaki, Phys. Rev. D **74**, 074018 (2006) [hep-ph/0609083]. D. Boer, A. Utermann and E. Wessels, Phys. Lett. B **671**, 91 (2009) [arXiv:0811.0998 [hep-ph]].
- [54] Z. -B. Kang and F. Yuan, Phys. Rev. D **84**, 034019 (2011) [arXiv:1106.1375 [hep-ph]].
- [55] Y. V. Kovchegov and M. D. Sievert, Phys. Rev. D **86**, 034028 (2012) [Erratum-ibid. D **86**, 079906 (2012)] [arXiv:1201.5890 [hep-ph]].
- [56] Z. -B. Kang and B. -W. Xiao, Phys. Rev. D **87**, 034038 (2013) [arXiv:1212.4809 [hep-ph]].
- [57] J. F. Owens, Rev. Mod. Phys. **59**, 465 (1987).
- [58] K. J. Golec-Biernat and M. Wusthoff, Phys. Rev. D **59**, 014017 (1998) [hep-ph/9807513].
- [59] A. Airapetian *et al.* [HERMES Collaboration], Phys. Lett. B **684**, 114 (2010) [arXiv:0906.2478 [hep-ex]].
- [60] D. Boer, Phys. Rev. D **60**, 014012 (1999).